A Novel Treatment Planning Design for Intraoperative Electron Radiation Therapy (IOERT) using an Electronic Board

Zahra Pouyanrad[1], Mojtaba Shamsaei Zafarghandi[2], Saeed Setayeshi[2]*

[1]PhD Candidate, Department of Energy Engineering and Physics, Amirkabir University of Technology, Tehran, Iran
[2]PhD, Department of Energy Engineering and Physics, Amirkabir University of Technology, Tehran, Iran

ABSTRACT

Background: Intraoperative Irradiation Therapy (IORT) refers to the delivery of radiation during surgery and needs the computed- thickness of the target as one of the most significant factors.

Objective: This paper aimed to compute target thickness and design a radiation pattern distributing the irradiation uniformly throughout the target.

Material and Methods: The Monte Carlo code was used to simulate the experimental setup in this simulation study. The electron flux variations on an electronic board's metallic layer were studied for different thicknesses of the target tissue and validated with experimental data of the electronic board.

Results: Based on the electron number for different Poly Methyl Methacrylate (PMMA) phantom thicknesses at various energies, 6 MeV electrons are suitable to determine the target thickness. Uniformity in radiation and corresponding time for each target were investigated. The iso-dose and percentage depth dose curves show that higher energies are suitable for treatment and distribute uniform radiation throughout the target. Increasing the phantom thickness leads to rising radiation time based on the radiation time corresponding to these energies. The tissue thickness of each section is determined, and the radiation time is managed by scanning the target.

Conclusion: Calculation of the thickness of the remaining tissue and irradiation time are needed after incomplete tumor removal in IORT for various remaining tissues. The patients should be protected from overexposure to uniform irradiation of tissues since the radiation dose is prescribed and checked by an oncologist.

Keywords

Intraoperative Radiotherapy; Radiation Therapy; Radiosurgery; Monte Carlo Method; Radiotherapy Dosage

Introduction

Intraoperative Radiation Therapy (IORT) is a specific method that may transfer sufficient and monotonous high-dose radiation to the tumor bed during surgery [1-4]. This treatment method decreases local recurrence risk, and healthy tissue receives a minor dose due to its localized radiation [5,6]. The physician's serious effort is impressively sending an intensive dose to the desired tissue while decreasing damage to healthy tissues surrounding the region of interest [7,8]. Today, mobile electron accelerators prepare new investigative fields for IORT [9].

The international society of intraoperative radiation therapy (ISIORT)

*Corresponding author: Saeed Setayeshi
Department of Energy Engineering and Physics, Amirkabir University of Technology, Tehran, Iran
E-mail: setayeshi.aut@gmail.com

Received: 26 September 2021
Accepted: 19 May 2022

reports that 20% of patients under IORT treatment are men, and the rest are women, with an average age of 60 years [10]. IORT is a convenient way of enhancing the colon and rectal cancer dose [11], suggested as a confident selection of treatment for a patient with regressive rectal cancer [12]. In addition, IORT, combined with chemotherapy and External Beam Radiation Therapy (EBRT) with the aim of dose escalation, improves the chance of overall survival and controls disease [13]. Also, IORT, along with EBRT, creates the best control rate for soft-tissue sarcoma (STS), which is better for local toxicity [11]. In addition, the accomplished investigations offer IORT as a secure alternative to whole breast radiotherapy (WBRT) [14-16].

One of the most common methods in IORT is Intraoperative Radiation Therapy with Electrons (IOERT) [17], in which the electrons are emitted with various energy ranges generated by mobile electron accelerators [2,18]. Furthermore, IOERT can adjust the treatment indicator due to the direct imagination capability of tumor volume [19,20]. In addition, Accelerated Partial Breast Irradiation (APBI) employs IOERT for low-risk breast cancers [21].

Some essential features of IORT, such as eliminating the gap between surgery and radiation therapy, reducing radiation-induced toxicity [22], and using an applicator to remove normal tissues from the irradiation regions, led to many studies on this treatment. Protection systems, such as shielding disks, cause the protection of underlying tissues from irradiation [23-25]. However, the required treatment time for IORT is lesser than external beam radiation therapy (EBRT) [26,27]; the IORT is more cost-effective than the EBRT [28-30]. In addition, the IORT adjusts the radiation to the tumor tissue and declines local effects in inoperable cancers [31], diminishing the renewed cancer risk [32].

The high accuracy in measurements of the target tissue thickness, determining the primary electron energy, can modify the IORT function. Moreover, the thickness of target tissue with unacceptable is measured using a needle [33]; intraoperative ultrasound is another method to specify the thickness [2,15,23]. A novel electronic board was designed to determine the thickness of target tissue based on measuring the electron flux at the board with an accuracy better than the others [5]. This study aimed to investigate a method to compute the thickness of target tissue in the IORT routine. Radiotherapists can calculate a good irradiation time based on the obtained thickness of the target tissue.

Material and Methods

Various simulated components were investigated in this simulation study, such as a 31.5 cm^2 circular electronic board composed of 16 pixels. In addition, a Monte Carlo simulation was also conducted using a Poly Methyl Methacrylate (PMMA) phantom and various electron energy sources with Monte Carlo N-Particle Transport (MCNP) code.

Electronic board

The electronic board's accumulated electron can determine the target tissue's thickness. Then, according to transferring the current from the board to an amplifier, recording, and processing the resulting signal, the desired information can be extracted. This system consists of two separate sections: 1) the electrical circuit in the path of electron irradiation acting as a sensor, and 2) the computer software analyzes data.

Each board pixel had a metal plate, detecting the electron flux with the thickness of 33 µm, 90% Tin,7% Copper, and 3% PVC. Each pixel with its circuit amplified the signal with a Bipolar Junction Transistor (BJT) transistor. In addition, the microcontroller for this circuit was from the DSPIC (Digital signal peripheral interface controller) family. The metal plate of each pixel of the board absorbed the flux of electrons and then converted it into its corresponding signals. The amplitude of this signal

was different for each thickness of the target. The outcome of the board was recorded and processed using executable software that connects to a computer via a USB port [5]. The electronic board image is shown in Figure 1.

Shielding disk

A protecting disk was used for the healthy tissues placed behind the disk from radiation and removed sensitive tissue from the beam. A double-format layer is a usual type of shielding disk. The initial layer minimized the back-scattered radiations with low atomic number (z), and the underneath layer absorbed the high-energy electrons with high-z [20,34]. In this simulation, the shielding disk was composed of a 3 mm PMMA as a low-z layer and a 3 mm stainless steel as a high-z layer.

Phantoms

In this research, different tissues were selected for phantom simulation. The simulation was conducted with the same phantom since the electronic board outcome was obtained using PMMA phantom with 1.190 g/cm^3 density. In the next step, three tissue phantoms are simulated: tumor, soft, and adipose tissue.

Monte Carlo Simulation

Monte Carlo (MC) is a good and robust technique to present electron flux distribution for different target thicknesses and radiation transportation simulation [14]. The MC code simulating various factors, such as heterologous materials, back scattered events, and beam-hardening [35] is one of the accurate computational techniques in medical and radiation physics fields and the treatment planning processing [36]. In addition, the results of MC code were used for validating treatment problems in radiotherapy fields [34].

The current study aimed to investigate the capability of an electrical system for measuring the thickness of the target tissue exposed to radiation. The flux received by the metal layer of the electronic board was proportional to the amplitude of the board signals in different thicknesses. In the MC code, tally f2 can compute the flux or counts of electrons for every target thickness and energy. The dose rate and the radiation time are calculated using Equations 1 and 2.

$$\dot{D} = \frac{\varphi\left(\text{count}/\text{cm}^2\right)\times \text{E}\left(\text{MeV}\right)\times 1.6\times 10-13\left(\text{J}/\text{MeV}\right)\times \text{S}\left(\text{cm}^2\right)}{\rho\left(\frac{Kg}{cm^3}\right)\times\left(sd\right)\left(cm^3\right)} \quad (1)$$

$$T = D_{measured} / \dot{D}_{calculated} \quad (2)$$

In Equation (1) φ is the rate of electron flux, E is the electron energy, S is the surface exposed to radiation, ρ is the phantom density, and d is the phantom thickness. The $D_{measured}$ in

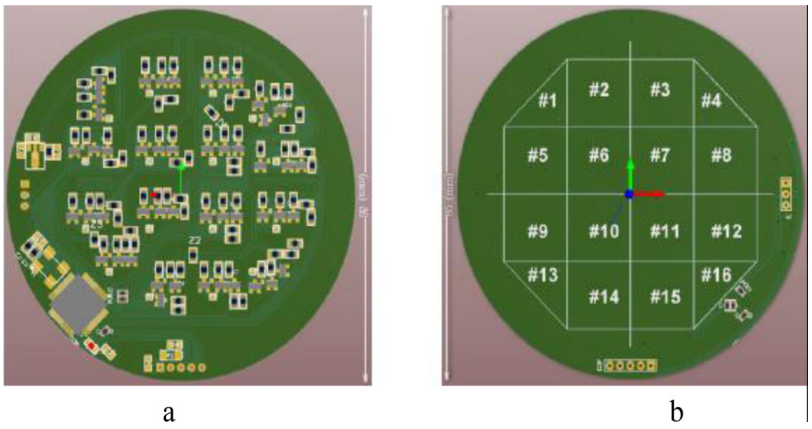

a b

Figure 1: Designed electronic board a) behind of board and b) front of the board (Reproduced from Yazdani MR et al. Nuclear Instruments and Methods in Physics Research Section A: Accelerators, Spectrometers, Detectors, and Associated Equipment. 2017;855: 32-7. [5])

Equation 2 is the amount of required dose for treatment of the target.

Results

Mont-Carlo calculation of thickness and validation by the electronic board result

The MC simulation results for different PMMA phantom thicknesses are shown in Figure 2 and Table 1 for all nominal energies. The outcome of the electronic board, which was experimentally obtained using a LIAC (linear accelerator) mobile accelerator in Khatam Hospital, Tehran, Iran was illustrated in Figure 3 and Table 2 to validate the simulation findings. This accelerator, equipped with a PMMA applicator with 0.5 (cm) thickness, worked in $\pi/2$ mode at 2.998 GHz and included 19 cavities with a 92.5 (cm) length. The magnetron producing the radiofrequency power for this accelerator was MG6090. The simulation and experiment results show an identical manner and reasonably good agreement.

Figure 4 presents the electron count for various tissues: adipose, soft, and tumor in 6 MeV energy. According to the results, there were no significant differences among different tissues.

Time determination for uniform target irradiation

Four Iso-dose curves of 6, 8, 10, and 12 MeV energies were constructed for a target thickness of 2.5 cm (Figure 5) to achieve a uniform

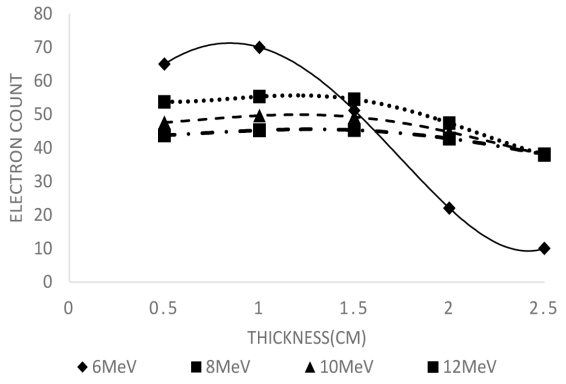

Figure 2: Monte Carlo simulation results for various electron source energies

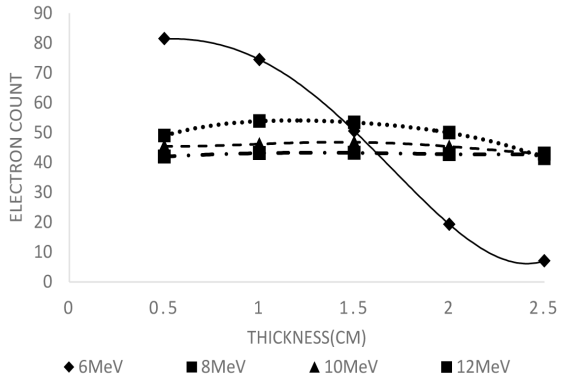

Figure 3: Electronic board outcome for Poly Methyl Methacrylate (PMMA) phantom

Table 1: Electron counts of Monte Carlo simulation for different thicknesses and energies

Thickness (cm)	Energies (MeV)			
	6 MeV	8 MeV	10 MeV	12 MeV
0.5	65	53.75	47.6	43.74
1	70	55.28	49.62	45.25
1.5	51.15	54.48	49.2	45.3
2	22	47.4	44.72	42.78
2.5	10	38.03	37.86	38

Table 2: Electron count of an electronic board for different thicknesses and energies

Thickness (cm)	Energies (MeV)			
	6 MeV	8 MeV	10 MeV	12 MeV
0.5	81.48	49	45.5	42
1	74.51	53.85	46.19	43.1237
1.5	50.5	53.44	46.8	43.23
2	19.25	49.96	45.37	42.81
2.5	7	41.38	42.91	42.92

dose distribution in treatment by electron radiation. However, the electrons with lower energy have a non-uniform dose distribution; the dose is more uniformly distributed at higher energies along with the thickness of the target. In addition, the percentage depth dose (PDD) curves also confirm this behavior (Figure 6).

The dose rate and radiation time were calculated using Equations 1 and 2, respectively. In Table 3, the simulation and experimental radiation time are reported, and Figure 7 reveals the radiation time of various target thicknesses for three energies (8, 10, and 12 MeV).

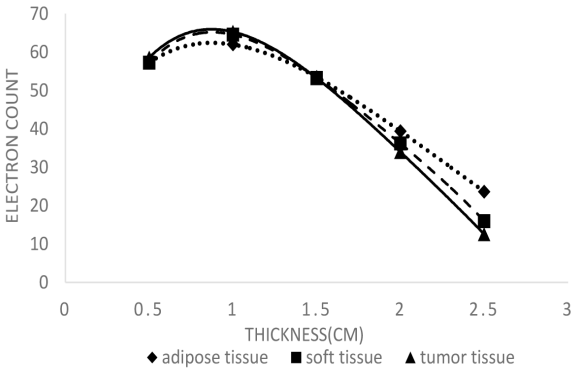

Figure 4: Electron flux for three types of tissues in 6 MeV energy

Discussion

In the first treatment step by IORT, the thickness of the target tissue has to be measured [33] using the emerged electron flux from the target tissue instead of a needle [5]. In this study, the MC simulation was used due to the the importance of code for simulating and exploring the beam interactions [36] and its accuracy in the treatment planning [34].

The results of MC simulation (Figure 2) and electronic board output (Figure 3) show that the electron count varies for different electron energies by changing the tissue thickness. For higher energies, these variations are small compared to 6 MeV electrons.

Figure 4 illustrates the simulation for different types of target tissues, in which can be

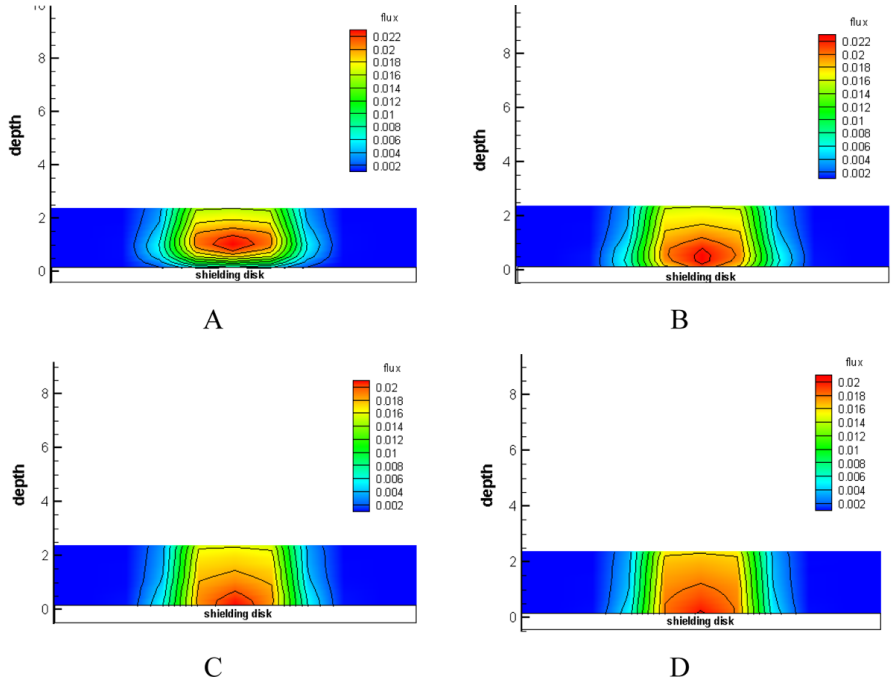

Figure 5: Iso-dose distribution for different energies in 2.5 (cm) of the target tissue. A) iso-dose for 6 MeV electron, B) iso-dose for 8 MeV electron, C) iso-dose for 10 Mev electron, and D) iso-dose for 12 MeV

only one type of tissue in the radiation due to unnoticeable differences in electron count for various tissues. Therefore, the depth of target tissue as an important factor of IOERT [5] was precisely calculated by scanning the target using a pencil beam, and electron flux emerged from the target.

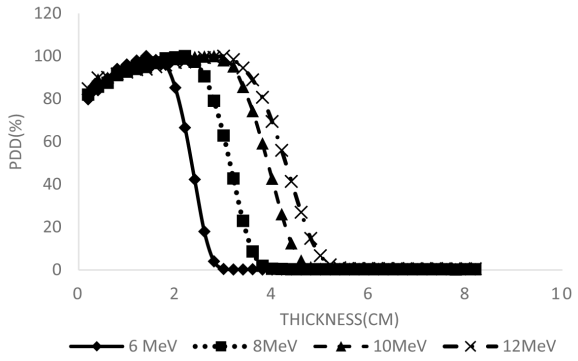

Figure 6: The percentage depth dose (PDD) at different electron energies

After determining the target thickness, a radiation pattern distributing the dose uniformly throughout the target tissue must be designed. Figure 5 shows that electrons with higher energy are better in treatment. Due to the different thicknesses of the target tissue, the right energy for treatment [37] and the irradiation time are managed.

In this study, a dose prescription of 21 Gy ($D_{measured}$) for a breast tissue with 2 (cm) thick irradiated in 104 s with 8 MeV electrons was used as a reference for a uniform treatment since the typical maximum thickness is about 2.5 (cm). First, the PMMA was considered equivalent to the tissue, and then the amount of dose rate was computed using Equation 1 to calculate the irradiation time of different tissue thicknesses.

Therefore, the dose rate for various phantom thicknesses can be calculated for each energy. The radiation time can be derived from Equa-

Table 3: Dose and radiation time for different thicknesses of Poly Methyl Methacrylate (PMMA) phantom and energies

Energy (MeV)	Thickness (cm)	Dose (GY/second)		Time(second)	
		experiment	simulation	experiment	simulation
8	0.5	0.807	0.899	26.02	23.36
	1	0.403	0.462	52.1	45.45
	1.5	0.269	0.303	78.1	69.31
	2	0.202	0.198	104	106.06
	2.5	0.161	0.13	130.4	161.54
10	0.5	1.01	0.941	20.8	22.32
	1	0.504	0.483	41.7	43.48
	1.5	0.336	0.326	62.5	64.42
	2	0.252	0.234	83.33	89.74
	2.5	0.202	0.158	104	132.91
12	0.5	1.211	1.097	17.34	19.14
	1	0.605	0.567	34.7	37.04
	1.5	0.403	0.378	52.1	55.55
	2	0.303	0.268	69.31	78.36
	2.5	0.242	0.19	86.8	110.53

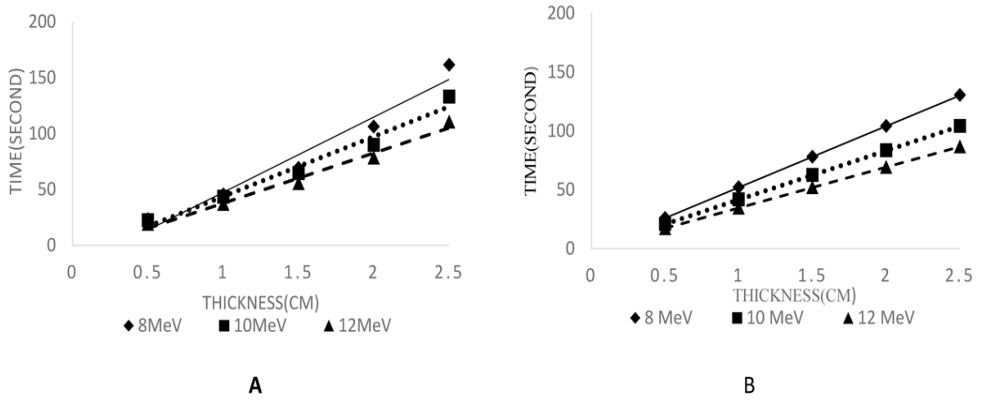

Figure 7: Radiation time vs. phantom thickness for different electron energies. A) calculated radiation time from simulation data and B) empirical radiation time.

tion 2 for all thicknesses and energies. In Table 3, the radiation time for five selected thicknesses is reported for different electron energies, and the radiation time for each arbitrary thickness can be estimated by using Figure 7.

The radiation time was presented using both simulation and experimental methods. According to Figure 7 and Table 3, the simulation results have an acceptable agreement. According to Figure 7, the time of radiation can decline with decreasing the target tissue thickness and be predicted for different thicknesses. Therefore, a decision-making system can be proposed for this LIAC accelerator. In the first step, the thickness of the target based on the pixel was determined and in the second step, the system read the radiation time of this thickness for selected energy. After the predicted time, the electronic board gives feedback to the accelerator head to move and check the next pixel.

Therefore, the electrical board signal amplitude would almost be the same at each depth, and the dose would be uniformly distributed in the target tissue using this diagram.

Conclusion

In IOERT, the geometry of the target tissue changes when the surgeon operates on the patient and removes the tumor. Therefore, no information is given about the thicknesses of the target tissues. This study introduced a new technique for determining the thickness of target tissue in IOERT. An MC simulation was performed to confirm the electrical board's results; therefore, an electrical board's response can measure the thicknesses of the possible remaining section of tissue using a 6 MeV electron pencil beam. Treatment time and uniformity in dose distribution throughout the target can be achieved using measured thicknesses with higher energy electrons. All parts of the target are simultaneously irradiated regardless of the remaining tissue depth in the IORT, resulting in the radiation oncologist finding out the target tissue thicknesses under irradiation and avoiding long time irradiation of the target with lower thicknesses.

Acknowledgment

I would like to express my great appreciation to Dr. Nahid Nafisi for her assistance in our research.

Authors' Contribution

M. Shamsaei Zafarghandi and S. Setayeshi propounded the idea. The method performance was conducted out by Z. Pouyanrad. The Results analysis was also performed by Z. Pouyanrad, M. Shamsaei Zafarghandi and S. Setayeshi. The research work was corrected and supervised by M. Shamsaei Zafarghandi and S. Setayeshi. All the authors read, modified, and approved the final version of the manuscript.

Ethical Approval

Ethical approval is not required since the electronic board was experimentally tested by PMMA phantom, and the simulation was done for different phantom thicknesses.

Informed consent

This is a teamwork faculty research group, and the built electronic board belongs to Dr. Saeed Setayeshi.

Conflict of Interest

None

References

1. Heidarloo N, Baghani HR, Aghamiri SM, Mahdavi SR, Akbari ME. Commissioning of beam shaper applicator for conformal intraoperative electron radiotherapy. *Appl Radiat Isot*. 2017;**123**:69-81. doi: 10.1016/j.apradiso.2017.02.039. PubMed PMID: 28260609.
2. Sedlmayer F, Reitsamer R, Wenz F, Sperk E, Fussl C, Kaiser J, et al. Intraoperative radiotherapy (IORT) as boost in breast cancer. *Radiat Oncol*. 2017;**12**(1):23. doi: 10.1186/s13014-016-0749-9. PubMed PMID: 28103903. PubMed PMCID: PMC5244574.
3. Roeder F, Alldinger I, Uhl M, Saleh-Ebrahimi L, Schimmack S, Mechtersheimer G, et al. Intraoperative Electron Radiation Therapy in Retroperitoneal Sarcoma. *Int J Radiat Oncol Biol Phys.* 2018;**100**(2):516-27. doi: 10.1016/j.ijrobp.2017.10.034. PubMed PMID: 29353660.
4. Islam MR, Watabe H, Stefano A. Measurement and Comparison of Output Factors Using Two Detectors for NOVAC7 IntraOperative Radiotherapy Accelerator. *IJMPCERO.* 2020;**9**(2):52-61. doi: 10.4236/ijmpcero.2020.92006.
5. Yazdani MR, Setayeshi S, Arabalibeik H, Akbari ME. Design, construction and performance evaluation of the target tissue thickness measurement system in intraoperative radiotherapy for breast cancer. *Nuclear Instruments and Methods in Physics Research Section A: Accelerators, Spectrometers, Detectors and Associated Equipment*. 2017;**855**:32-7. doi: 10.1016/j.nima.2016.12.065.
6. Malter W, Kirn V, Richters L, Fridrich C, Markiefka B, Bongartz R, et al. Intraoperative Boost Radiotherapy during Targeted Oncoplastic Breast Surgery: Overview and Single Center Experiences. *Int J Breast Cancer*. 2014;**2014**:637898. doi: 10.1155/2014/637898. PubMed PMID: 25587453. PubMed PMCID: PMC4281395.
7. Falco M, Masojć B, Milchert-Leszczyńska M, Kram A. Frequency of whole breast irradiation (WBRT) after intraoperative radiotherapy (IORT) is strongly influenced by institutional protocol qualification criteria. *Rep Pract Oncol Radiother*. 2018;**23**(1):34-8. doi: 10.1016/j.rpor.2017.11.003. PubMed PMID: 29270082. PubMed PMCID: PMC5735296.
8. Willett CG, Czito BG, Tyler DS. Intraoperative radiation therapy. *J Clin Oncol.* 2007;**25**(8):971-7. doi: 10.1200/JCO.2006.10.0255. PubMed PMID: 17350946.
9. Esposito A, Sakellaris T, Limede P, Costa F, Cunha LT, Dias AG, Lencart J, Sarmento S, Rosa CC. Effects of shielding on pelvic and abdominal IORT dose distributions. *Phys Med*. 2016;**32**(11):1397-404. doi: 10.1016/j.ejmp.2016.10.004. PubMed PMID: 27780674.
10. Krengli M, Calvo FA, Sedlmayer F, Sole CV, Fastner G, Alessandro M, et al. Clinical and technical characteristics of intraoperative radiotherapy. *Strahlenther Onkol.* 2013;**189**(9):729-37. doi: 10.1007/s00066-013-0395-1. PubMed PMID: 23842635.
11. Haddock MG. Intraoperative radiation therapy for colon and rectal cancers: a clinical review. *Radiat Oncol.* 2017;**12**(1):11. doi: 10.1186/s13014-016-0752-1. PubMed PMID: 28077144. PubMed PMCID: PMC5225643.
12. Moradi F, Ung NM, Khandaker MU, Mahdiraji GA, Saad M, Abdul Malik R, et al. Monte Carlo skin dose simulation in intraoperative radiotherapy of breast cancer using spherical applicators. *Phys Med Biol*. 2017;**62**(16):6550-66. doi: 10.1088/1361-6560/aa7fe6. PubMed PMID: 28708603.
13. Roeder F, Krempien R. Intraoperative radiation therapy (IORT) in soft-tissue sarcoma. *Radiat Oncol.* 2017;**12**(1):20. doi: 10.1186/s13014-016-0751-2. PubMed PMID: 28100249. PubMed PMCID: PMC5244699.
14. Silverstein MJ, Epstein M, Kim B, Lin K, Khan S, Snyder L, et al. Intraoperative Radiation Therapy (IORT): A Series of 1000 Tumors. *Ann Surg Oncol.* 2018;**25**(10):2987-93. doi: 10.1245/s10434-018-6614-3. PubMed PMID: 29968030.
15. Silverstein MJ, Epstein MS, Lin K, Chen P, Khan S, Snyder L, et al. Intraoperative Radiation Using Low- Kilovoltage X-Rays for Early Breast Cancer: A Single Site Trial. *Ann Surg Oncol*. 2017;**24**(10):3082-7. doi: 10.1245/s10434-017-5934-z. PubMed PMID: 28766211.

16. Lorenzen AW, Kiriazov B, De Andrade JP, Lizarraga IM, Scott-Conner CE, Sugg SL, et al. Intraoperative Radiotherapy for Breast Cancer Treatment in a Rural Community. *Ann Surg Oncol*. 2018;**25**(10):3004-10. doi: 10.1245/s10434-018-6574-7. PubMed PMID: 30030731. PubMed PMCID: PMC6357224.
17. Kaiser J, Reitsamer R, Kopp P, Gaisberger C, Kopp M, Fischer T, et al. Intraoperative Electron Radiotherapy (IOERT) in the Treatment of Primary Breast Cancer. *Breast Care (Basel).* 2018;**13**(3):162-7. doi: 10.1159/000489637. PubMed PMID: 30069175. PubMed PMCID: PMC6062668.
18. Gunderson LL, Willett CG, Calvo FA. Intraoperative Irradiation: Techniques and Results. 2nd Edition. Humana Press: 2011.
19. López-Tarjuelo J, Bouché-Babiloni A, Morillo-Macías V, Santos-Serra A, Ferrer-Albiach C. Practical issues regarding angular and energy response in in vivo intraoperative electron radiotherapy dosimetry. *Rep Pract Oncol Radiother.* 2017;**22**(1):55-67. doi: 10.1016/j.rpor.2016.09.009. PubMed PMID: 27790075. PubMed PMCID: PMC5072178.
20. Robatjazi M, Baghani HR, Mahdavic SR, Felici G. Evaluation of dosimetric properties of shielding disk used in intraoperative electron radiotherapy: A Monte Carlo study. *Appl Radiat Isot.* 2018;**139**:107-13. doi: 10.1016/j.apradiso.2018.04.037. PubMed PMID: 29751323.
21. Struikmans H, Snijders M, Mast ME, Fisscher U, Franssen JH, Immink MJ, et al. Single dose IOERT versus whole breast irradiation: Cosmetic results in breast-conserving therapy. *Strahlenther Onkol*. 2016;**192**(10):705-13. doi: 10.1007/s00066-016-1029-1. PubMed PMID: 27538776.
22. Harris EER, Small W Jr. Intraoperative Radiotherapy for Breast Cancer. *Front Oncol.* 2017;**7**:317. doi: 10.3389/fonc.2017.00317. PubMed PMID: 29312887. PubMed PMCID: PMC5743678.
23. Matsumine A, Tsujii M, Nakamura T, Asanuma K, Matsubara T, Kakimoto T, et al. Minimally invasive surgery using intraoperative electron-beam radiotherapy for the treatment of soft tissue sarcoma of the extremities with tendon involvement. *World J Surg Oncol.* 2016;**14**(1):214. doi: 10.1186/s12957-016-0968-4. PubMed PMID: 27514518. PubMed PMCID: PMC4982423.
24. Castro Neto AJ, Haddad CM, Pelosi EL, Zevallos- Chávez JY, Yoriyaz H, Siqueira PD. Monte Carlo simulation as an auxiliary tool for electron beam quality specification for intra-operative radiotherapy. *Braz J Phys*. 2005;**35**(3B):801-4. doi: 10.1590/S0103-97332005000500021.
25. Nevelsky A, Bernstein Z, Bar-Deroma R, Kuten A, Orion I. Design and dosimetry characteristics of a commercial applicator system for intra-operative electron beam therapy utilizing ELEKTA Precise accelerator. *J Appl Clin Med Phys*. 2010;**11**(4):3244. doi: 10.1120/jacmp.v11i4.3244. PubMed PMID: 21081880. PubMed PMCID: PMC5720419.
26. Bhandari T, Babaran W, Forouzannia A, Williams V, Harness J, Carpenter M, e al. A prospective phase I comparison of toxicity and cosmesis outcomes of single-fraction IORT and hypofractionated radiotherapy with IORT boost in early-stage breast cancer. *Brachytherapy.* 2017;**16**(6):1232-8. doi: 10.1016/j.brachy.2017.09.002. PubMed PMID: 29032999.
27. Mourtada F. Physics of intraoperative radiotherapy for the breast. In: Arthur DW, Vicini FA, Wazer DE, Khan AJ. Short course breast radiotherapy; Springer, Cham; 2016. p. 317-25.
28. Patel R, Ivanov O, Voigt J. Lifetime cost-effectiveness analysis of intraoperative radiation therapy versus external beam radiation therapy for early stage breast cancer. *Cost Eff Resour Alloc.* 2017;**15**:22. doi: 10.1186/s12962-017-0084-5. PubMed PMID: 29151818. PubMed PMCID: PMC5679386.
29. Hedie M, Zahra K, Khosro K, Majid A, Maryam S. Cost-effectiveness of radiotherapy during surgery compared with external radiation therapy in the treatment of women with breast cancer. *JHMI*. 2016;3(2):33-8.
30. Alvarado MD, Mohan AJ, Esserman LJ, Park CC, Harrison BL, Howe RJ, et al. Cost-effectiveness analysis of intraoperative radiation therapy for early-stage breast cancer. *Ann Surg Oncol.* 2013;**20**(9):2873-80. doi: 10.1245/s10434-013-2997-3. PubMed PMID: 23812769.
31. Zaki Azzam A, Alqarni A, Mahmoud Amin T. The role of intraoperative radiotherapy (IORT) in the management of patients with pancreatic and periampullary cancer: A single center experience. *J Egypt Natl Canc Inst.* 2018;30(2):77-9. doi: 10.1016/j.jnci.2018.03.002. PubMed PMID: 29680448.
32. Woolf DK, Williams NR, Bakshi R, Madani SY, Eaton DJ, Fawcitt S, et al. Biological dosimetry for breast cancer radiotherapy: a comparison of external beam and intraoperative radiotherapy. *Springerplus*. 2014;**3**:329. doi: 10.1186/2193-1801-3-329. PubMed PMID: 25045612. PubMed PMCID: PMC4093905.
33. Barros AC, Hanna SA, Carvalho HA, Martella E, Andrade FE, Piato JR, Bevilacqua JL. Intraop-

erative full-dose of partial breast irradiation with electrons delivered by standard linear accelerators for early breast cancer. *Int J Breast Cancer*. 2014;**2014**:568136. doi: 10.1155/2014/568136. PubMed PMID: 25587452. PubMed PMCID: PMC4281392.

34. Catalano M, Agosteo S, Moretti R, Andreoli S. Montecarlo simulation code in optimisation of the IntraOperative Radiation Therapy treatment with mobile dedicated accelerator. First European Workshop on Monte Carlo Treatment Planning; Gent, Belgium: IOP Publishing; 2007.
35. Herranz E, Herraiz JL, Cal-González J, Corzo PM, Guerra P, Udias JM. Iterative reconstruction of whole accelerator phase spaces for Intraoperative Radiation Therapy (IORT) from measured dose data. In 2011 IEEE Nuclear Science Symposium Conference Record; Valencia, Spain: IEEE; 2011. p. 2644-6.
36. Mihailescu D, Borcia C. Monte Carlo simulation of the electron beams produced by a linear accelerator for intraoperative radiation therapy. *Romanian Reports in Physics.* 2014;**66**(1):61-74.
37. Vidali C, Severgnini M, Bellio G, Giudici F, Milan V, Pellin Z, et al. State of the art in breast intraoperative electron radiation therapy after intraoperative ultrasound introduction. *Radiol Oncol*. 2021;**55**(3):333-40. doi: 10.2478/raon-2021-0023. PubMed PMID: 33991470. PubMed PMCID: PMC8366729.